Journal of Solid State Chemistry 183 (2010) 304–309

Contents lists available at ScienceDirect

Journal of Solid State Chemistry

journal homepage: www.elsevier.com/locate/jssc

Synthesis and structural characterization of two cobalt phosphites: 1-D $(H_3NC_6H_4NH_3)Co(HPO_3)_2$ and 2-D $(NH_4)_2Co_2(HPo_3)_3$

Chi-Chang Cheng [a], Wei-Kuo Chang [a,*], Ray-Kuang Chiang [a], Sue-Lein Wang [b]

[a] Department of Material Science and Engineering, Far East University, Tainan 74448, Taiwan, China
[b] Department of Chemistry, National Tsing Hua University, Hsinchu, Taiwan 30013, China

ARTICLE INFO

Article history:
Received 24 February 2009
Received in revised form
26 October 2009
Accepted 29 October 2009
Available online 14 November 2009

Keywords:
Cobalt phosphites
Crystal structures

ABSTRACT

Two new cobalt phosphites, $(H_3NC_6H_4NH_3)Co(HPO_3)_2$ (**1**) and $(NH_4)_2Co_2(HPO_3)_3$ (**2**), have been synthesized and characterized by single-crystal X-ray diffraction. All the cobalt atoms of **1** are in tetrahedral CoO_4 coordination. The structure of **1** comprises twisted square chains of four-rings, which contain alternating vertex-shared CoO_4 tetrahedra and HPO_3 groups. These chains are interlinked with trans-1,4-diaminocyclohexane cations by hydrogen bonds. The 2-D structure of **2** comprises anionic complex sheets with ammonium cations present between them. An anionic complex sheet contains three-deck phosphite units, which are interconnected by Co_2O_9 to form complex layers. Magnetic susceptibility measurements of **1** and **2** showed that they have a weak antiferromagnetic interaction.

1. Introduction

Organically templated transition metal phosphates are of great interest because of their potential applications in catalysis, optical and electromagnetic functions, and synthesis of novel structures [1]. The structures of these compounds exhibit various architectures with zero-, one-, two-, and three-dimensional frameworks, which surround organic templates [2]. Most templates are protonated amine cations and present hydrogen bonds by $N–H—O_{framework}$. These hydrogen bonds play the following two important roles in structures: (1) they act as stabilizers of the resulting inorganic network and (2) they act as separate entities of inorganic networks. On the other hand, the building units of the framework are deeply influenced by the chosen transition metal polyhedra and the degree of protonation of the phosphate anions. For example, cobalt is a tetrahedrally coordinated atom in cobalt phosphates, which are usually zeolitic analogues. However, cobalt has high coordination flexibility and a strong tendency to form edge-sharing or face-sharing linkages of metal-oxygen polyhedra. These properties usually lead to difficulty in mimicking a zeolite-type structure, but can lead to the possibility of new structural morphology and interesting magnetic properties [3–8]. Recently, the HPO_3 group has been investigated as a possible replacement for the tetrahedral HPO_4 unit with great success [9–14]. It is interesting to note that some zinc phosphites are isostructural to the corresponding zinc mono hydrogen phosphates, whereas others exhibit novel structures [15–19].

In contrast to the various zinc phosphites that have been found, the structural chemistry of cobalt phosphites is relatively unexplored. There is only one alkaline cobalt phosphite, $Na_2Co(HPO_3)_2$, [20] two organically templated cobalt phosphites, $C_2H_{10}N_2Co_3(HPO_3)_4$, [21,22] and some organic/inorganic hybrid cobalt phosphites and mixed cobalt–zinc phosphites [23–26]. In order to extend our knowledge of cobalt phosphites, we conducted a study on their synthesis in the system of Co-HPO_3-amine(ammonium). Herein, we report the syntheses and structural characterization of two new compounds: one-dimensional $(H_3NC_6H_4NH_3)Co(HPO_3)_2$ (**1**) and two-dimensional $(NH_4)_2Co_2(HPO_3)_3$ (**2**).

2. Experimental

Syntheses. A reaction mixture of $CoCl_2 \cdot 6H_2O$ (1.0 mmol), H_3PO_3 (4.0 mmol), $Si(C_2H_5O)_4$ (0.5 mmol), trans-1,4-diaminocyclohexane (7.0 mmol), and distilled water (5.0 mL) was stirred for 30 min. It was then sealed in a Teflon-lined acid digestion bomb, heated to 160 °C for 3 days, and slowly cooled to room temperature at 6 °C h^{-1}. The final pH of the solution was 4.5. The resulting solid was filtered off and washed with distilled water. It consisted of **1** as the major product in the form of blue plane crystals together with some unidentified purple powders. The XRD pattern of the purified sample agreed well with that calculated from the single-crystal data (*vide infra*).

A reaction mixture of $Co(NO_3)_2 \cdot 6H_2O$ (1.0 mmol), H_3PO_3 (4.0 mmol), ammonium hydroxide (25%, 4.0 mmol), Urea (1.0 mmol), HF (40%, 0.2 mL), and *n*-butanol (10.0 mL) was stirred

* Corresponding author.
E-mail address: cwk9146@cc.feu.edu.tw (W.-K. Chang).

0022-4596/$ - see front matter © 2009 Elsevier Inc. All rights reserved.
doi:10.1016/j.jssc.2009.10.029

for 30 min and then sealed in a Teflon-lined acid digestion bomb and heated to 160 °C for 3 days, followed by slow cooling to room temperature at 6 °C h^{-1}. The resulting solid was filtered off and washed with distilled water. It consisted of **2** as a pure product in the form of red rose crystals. The XRD pattern of the bulk sample agreed well with that calculated from single-crystal data (vide infra).

Single-crystal X-ray structure analysis. Crystals with dimensions of $0.20 \times 0.13 \times 0.06$ mm for **1** and $0.15 \times 0.15 \times 0.02$ mm for **2** were selected for indexing and intensity data collection at 295 K. Diffraction measurements were performed on a Bruker Smart-CCD diffractometer system equipped with a normal focus, 3 KW sealed-tube X-ray source (λ=0.71073 Å). Intensity data were collected in 1271 frames with increasing ω (0.3° per frame). The unit cell dimensions were determined by a least-squares fit of 600 refractions. The intensity data were corrected for Lorentz polarization and absorption effects. The absorption correction was based on symmetry-equivalent reflections, and it was applied using the SADABS program. On the basis of the systematic absences and intensity distribution statistics, space groups were determined to be *Pccn* and *P*-31*c* for **1** and **2**, respectively. Values of measured and observed reflections (Iobs > 2(*I*)) are 7647 and 3442 for **1** and **2**, respectively. Direct methods were used to locate Co, P, and a few oxygen and nitrogen atoms with the remaining non-hydrogen atoms found from successive difference Fourier maps. The thermal parameters and results of bond length were used to identify the carbon atoms in **1**. The atomic coordinates of all the H atoms in the organic amine molecules or the hydride in the phosphite were located directly on a difference map. Structural parameters for **1** and **2** were refined on the basis of F2. In the final cycle of refinement, the atomic coordinates and anisotropic thermal parameters of all the non-hydrogen atoms and the fixed atomic coordinates and isotropic thermal parameter of the hydrogen atoms converged at *R*=0.0295 and 0.0303 for **1** and **2**, respectively. Corrections for secondary extinction and anomalous dispersion were applied. The neutral-atom scattering factors for all the atoms were obtained from standard sources. All the calculations were performed using SHELXTL programs [27]. The crystallographic data are presented in Table 1. The final atomic coordinates and selected bond distances are individually presented in Tables 2 and 3, respectively.

We did our best to determine the space group and coordinate of P(2) in **2**. Three space groups (*P*31*c*, *P*63*m*, and $P\bar{3}1c$) were suggested by the SHELXTL program. All the three space groups can be used to refine the structure, and the final *R* values given by all three space groups were below 0.050. However, standard deviations of the bond lengths were unusually large, and many correlation matrix elements were revealed for both *P*31*c* and *P*63*m*. When using the space group of $P\bar{3}1c$, the coordinate of P(2) was in a special position (1/3, 1/3, 2/3), and its thermal parameter was unusually large (0.17649) at U33 along the [001] direction. This suggested that P(2) had a positional disorder at two sites along the [001] direction. Therefore, we put P(2) at both sites (1/3, 1/3, 2/3 ± 0.3) and began refining the structure again. The result of this refinement for P(2) was a reasonable value (0.01484) at U33 and a low final *R*.

Table 1
Crystallographic data for compounds **1**, and **2**.

	1	**2**
Formula	$C_6\ H_{18}\ Co\ N_2\ O_6\ P_2$	$H_{11}\ Co_2\ N_2\ O_9\ P_3$
fw	335.09	393.88
Space group	*Pccn*	$P\bar{3}1c$
a (Å)	17.0811(13)	5.3671(5)
b (Å)	8.5611(6)	5.3671(5)
c (Å)	8.7654(6)	18.750(3)
γ (deg)	90	120
V (Å^3)	1281.79(16)	467.75(9)
Z	4	2
No. refltn collected	7647	3140
T (K)	295(2)	295(2)
λ (Å)	0.71 073	0.71 073
ρcalcd (gcm^{-3})	1.736	2.797
μ (mm^{-1})	1.605	4.100
*R*1[a]	0.0295	0.0303
*wR*2[b]	0.0713	0.0799

[a] $R1 = \Sigma||F_o| - |F_c||/\Sigma|F_o|$.
[b] $wR2 = [\Sigma w(|F_o|^2 - |F_c|^2)^2]/\Sigma w(|F_o|^2)^2]^{1/2}$, $w = 1/[\square^2(F_o^2) + (0.0409P)^2]$ for 1, and $w = 1/[\square^2(F_o^2) + (0.0551P)^2 + 6.79P]$ for 2, where $P = (F_o + {}^2F_c^2)/3$.

Table 2
Atomic coordinates ($\times 10^4$) and thermal parameters (Å$^2 \times 10^3$) for **1** and **2**.

	x	*y*	*z*	*U* (eq)
1				
Co(1)	2500	2500	2326(1)	21(1)
P(1)	3457(1)	4450(1)	4846(1)	22(1)
O(1)	3367(1)	3321(2)	3523(2)	28(1)
O(2)	2813(1)	722(2)	1044(2)	29(1)
O(3)	3548(1)	6125(2)	4352(2)	39(1)
N(1)	3546(1)	8794(2)	6152(2)	25(1)
C(1)	4236(1)	9773(2)	5706(3)	23(1)
C(2)	4321(1)	9838(3)	3980(3)	31(1)
C(3)	5025(1)	10 851(3)	3546(3)	31(1)
2				
Co(1)	6667	3333	6717(1)	12(1)
P(1)	0	0	6286(1)	12(1)
P(2)	3333	−3333	7329(1)	11(1)
O(1)	3111(5)	1558(6)	6042(1)	22(1)
O(2)	4928(4)	−145(7)	7500	17(1)
N(1)	3333	−3333	5353(3)	20(1)

Table 3
Selected bond lengths (Å) and bond angles (°) for **1** and **2**.

Compound 1		**Compound 2**	
Co(1)–O(1)	1.9469(15)	Co(1)–O(1)#5	2.082(2)
Co(1)–O(1)#1	1.9469(15)	Co(1)–O(1)	2.082(2)
Co(1)–O(2)	1.9662(14)	Co(1)–O(1)#6	2.082(2)
Co(1)–O(2)#1	1.9662(14)	Co(1)–O(2)#5	2.184(3)
P(1)–O(3)	1.5060(16)	Co(1)–O(2)	2.184(3)
P(1)–O(1)	1.5169(15)	Co(1)–O(2)#6	2.184(3)
P(1)–O(2)#2	1.5285(17)	Co(1)–Co(1)#7	2.9365(14)
N(1)–C(1)	1.499(3)	P(1)–O(1)#8	1.517(2)
C(1)–C(3)#4	1.519(3)	P(1)–O(1)	1.517(2)
C(1)–C(2)	1.521(3)	P(1)–O(1)#9	1.517(2)
C(2)–C(3)	1.531(3)	P(2)–O(2)	1.516(3)
C(3)–C(1)#4	1.519(3)	P(2)–O(2)#10	1.516(3)
		P(2)–O(2)#11	1.516(3)
O(1)–Co(1)–O(1)#1	114.74(9)	O(1)#5–Co(1)–O(1)	86.85(9)
O(1)–Co(1)–O(2)	112.40(6)	O(1)#5–Co(1)–O(2)#5	96.64(8)
O(1)–Co(1)–O(2)#1	103.61(6)	O(1)–Co(1)–O(2)#5	175.22(9)
O(2)–Co(1)–O(2)#1	110.29(9)	O(1)–Co(1)–O(2)	96.64(8)
		O(2)#5–Co(1)–O(2)	79.74(9)

Symmetry transformations used to generate equivalent atoms: #1 $-x+1/2,-y+1/2,z$; #2 $x,-y+1/2,z+1/2$; #3 $x,-y+1/2,z-1/2$; #4 $-x+1,-y+2,-z+1$; #5 $-y+1,x-y,z$; #6 $-x+y+1,-x+1,z$; #7 $-y+1,-x+1,-z+3/2$; #8 $-x+y,-x,z$; #9 $-y,x-y,z$; #10 $-y,x-y-1,z$; #11 $-x+y+1,-x,z$.

3. Results and discussion

Structure of $(H_3NC_6H_4NH_3)Co(HPO_3)_2$. There are nine asymmetric non-hydrogen atoms in **1**, as shown in Fig. 1a. The

structure crystallizes in the space group of *Pccn* and consists of $Co(HPO_3)_2^{-2}$ anions and diprotonated trans-1,4 diaminocyclohexane cations. The $Co(HPO_3)_2^{-2}$ anion has a geometry of twisted square chains, in which each square is comprises alternately linked two CoO_4 tetrahedra and two HPO_3 groups. Each CoO_4 tetrahedron is corner-shared with four HPO_3 groups via O(1) and O(2), while each HPO_3 is linked to only two CoO_4 tetrahedra through the same O(1) and O(2). The pseudo-tetrahedral HPO_3 group also contains a short terminal P–O(3) bond (1.506 Å) and a P–H bond. The chains run along the [001] direction and are located on the intersection of the two c-glide planes perpendicular to the respective *a* and *b* axes, as shown in Fig. 2a. The symmetry between the chains is n-glide related, and the chains are interlinked through diprotonated trans-1,4-diaminocyclohexane cations by hydrogen bonds that are spread over the (110) and (1–10) planes, as shown in Fig. 2b. The hydrogen bond length and angle details are listed in Table 4.

Structure of $(NH_4)_2Co_2(HPO_3)_3$. There are six asymmetric non-hydrogen atoms in **2**, as shown in Fig. 1b. The structure crystallizes in the space group of $P\bar{3}1c$ and consists of $[Co_2(HPO_3)_3]^{-2}$ anions and NH_4^+ cations. The complex layer of $[Co_2(HPO_3)_3]^{-2}$ contains three decks of phosphite groups, where phosphite groups are interconnected by dimmeric Co_2O_9, as shown in Fig. 3. The HP(1)O_3 groups of the first deck and the third deck are related by $\bar{3}$ symmetry operations. The HP(2)O_3 groups in the middle deck are located on a three-fold rotation axis. P(2) is positionally disordered in two positions, which are located above

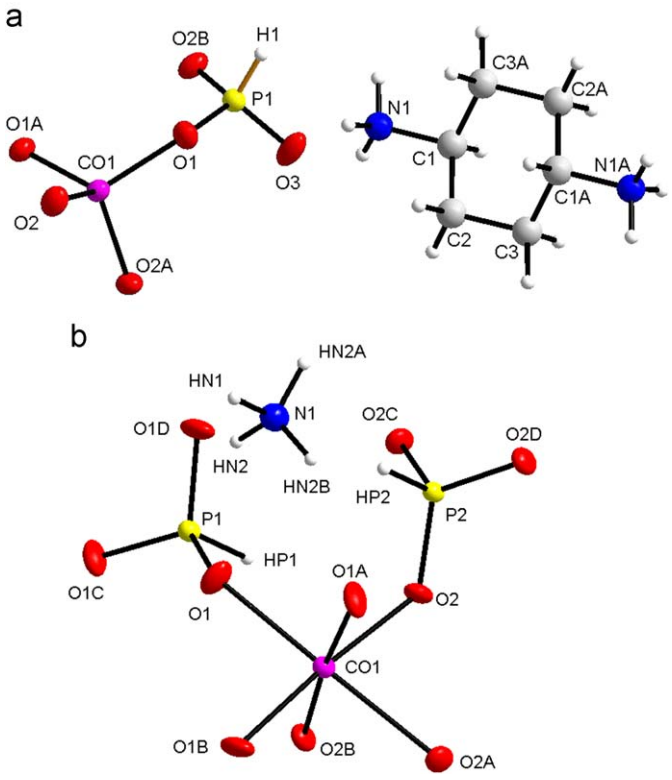

Fig. 1. The asymmetric units of (a) compound **1** and (b) compound **2**. Color code: P atoms, yellow; Co atoms, pink; C atoms, gray; N atoms, blue; H atoms, white. (For interpretation of the references to color in this figure legend, the reader is referred to the web version of this article.)

Table 4
Hydrogen bonds for **1** and **2**.

D–H···A	D–H (Å)	H···A (Å)	D_A (Å)	Angle (deg)
1				
N(1)–H(1B)···O(2)	0.933	1.943	2.849	163.2
N(1)–H(1B)···O(2)	1.001	1.825	2.806	165.8
N(1)–H(1D)···O(3)	0.903	1.897	2.776	164.3
2				
N(1)–HN(2)···O(1)	0.932	2.241	2.982	135.94
N(1)–HN(2)···O(1)	0.932	2.183	2.979	142.85

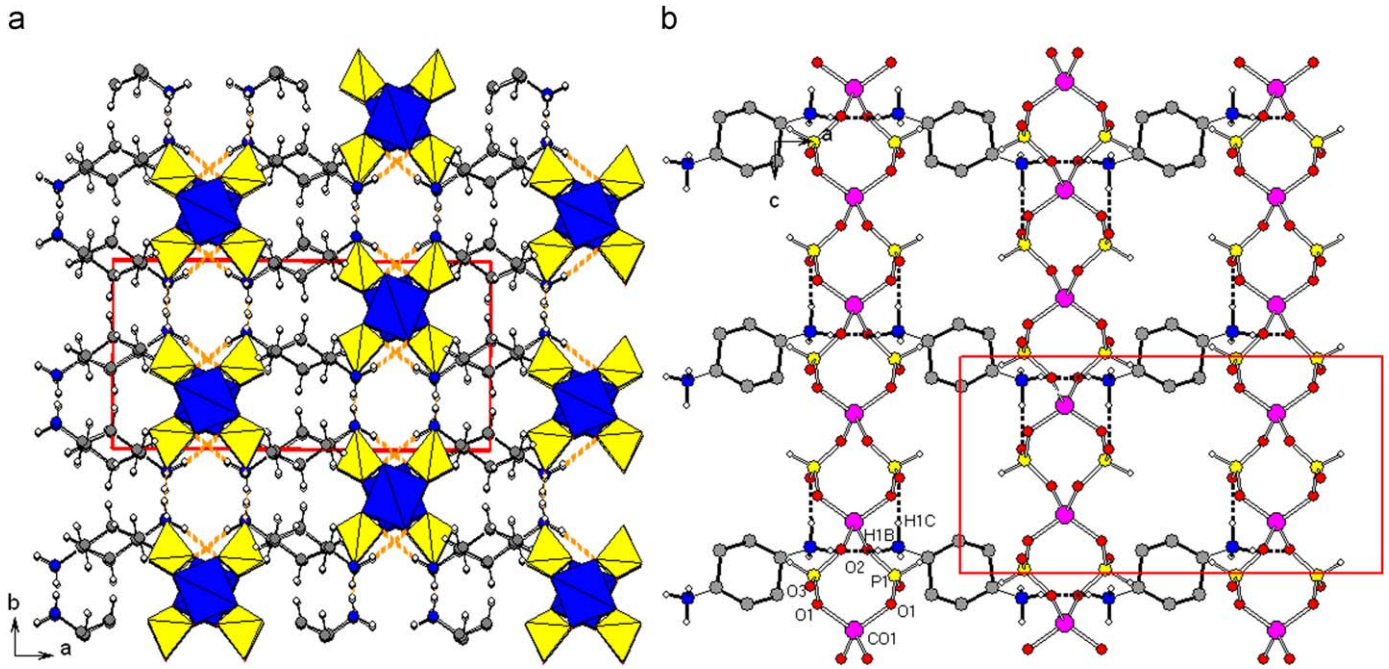

Fig. 2. Polyhedral view of **1** showing projection along [001] (a), and ball stick view showing projection along [010] (b). The yellow tetrahedra are represented as HPO_3 group and blue tetrahedral as CoO_4. Color code: P atoms, yellow; Co atoms, pink; C atoms, gray; N atoms, blue; the H atoms are open cycle. The dash lines represent hydrogen bonds. (For interpretation of the references to color in this figure legend, the reader is referred to the web version of this article.)

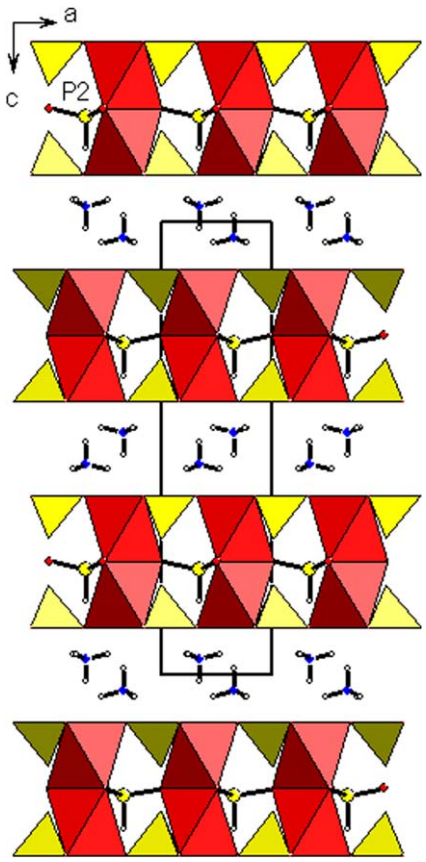

Fig. 3. Polyhedral view of **2** showing the projection along [010]. The yellow tetrahedra are represented as HPO_3 group and red octahedral as CoO_6. Color code: P atoms (a positional disorder at two sites along [001] direction.), yellow; O atoms, red; N atoms, blue; the H atoms are open cycle. (For interpretation of the references to color in this figure legend, the reader is referred to the web version of this article.)

or below the central mirror plane of the complex layers. Therefore, both these positions are probably half occupied. This was proven by the refinement of the unconstrained occupying factors for the two positions. The dimmeric $Co(1)_2O_9$ is composed of two face-shared CoO_6 octahedra. The $Co(1)_2O_9$ units are also located on the three-fold axis, and both the Co(1) ions are related by $\bar{1}$ symmetry operations. The Co–Co distance in the dimmeric Co_2O_9 is 2.9365 Å. The ammonium cations are present between the cobalt phosphite layers to compensate for the negative charge of these layers and are located at the center of the six-ring windows of the layers via the N–H···O hydrogen bonds, as shown in Fig. 4b. The hydrogen bond length and angle details are listed in Table 4.

4. Discussion

It is interesting to relate the structure building units of **1** and **2** to known cobalt phosphates and phosphites. In structural chemistry, the twisted square chain in **1** is a prototype unit comprising a zeolite-like porous structure. Many complex structures are created by a hydrolysis-condensation of this parent chain. Few examples of compounds having such structures include some aluminum phosphates reported by Ozin's group [28], zinc phosphates reported by Rao's group, [2] and transition metal phosphites [8]. This twisted square chain has also been found in a known cobalt phosphate, (R, S)-$(C_5H_{14}N_2)Co(HPO_4)_2$(**3**), [29] in which $(HPO_3)^{2-}$ and $(HPO_4)^{2-}$ can be viewed as equivalent species. Hydrogen bonds between the organic amine and the inorganic chain are shown in **1** and **3**. However, the interchain and intrachain hydrogen bonds are only shown in **3**. Because the HPO_3 group is a three-connector group and is not easily protonated, there is a low possibility of formation of a hydrogen bond between phosphite groups. Therefore, four-ring chains can be stabilized and freely suspended in tetrahedron-based metal phosphites, and 3-D structures, which comprise

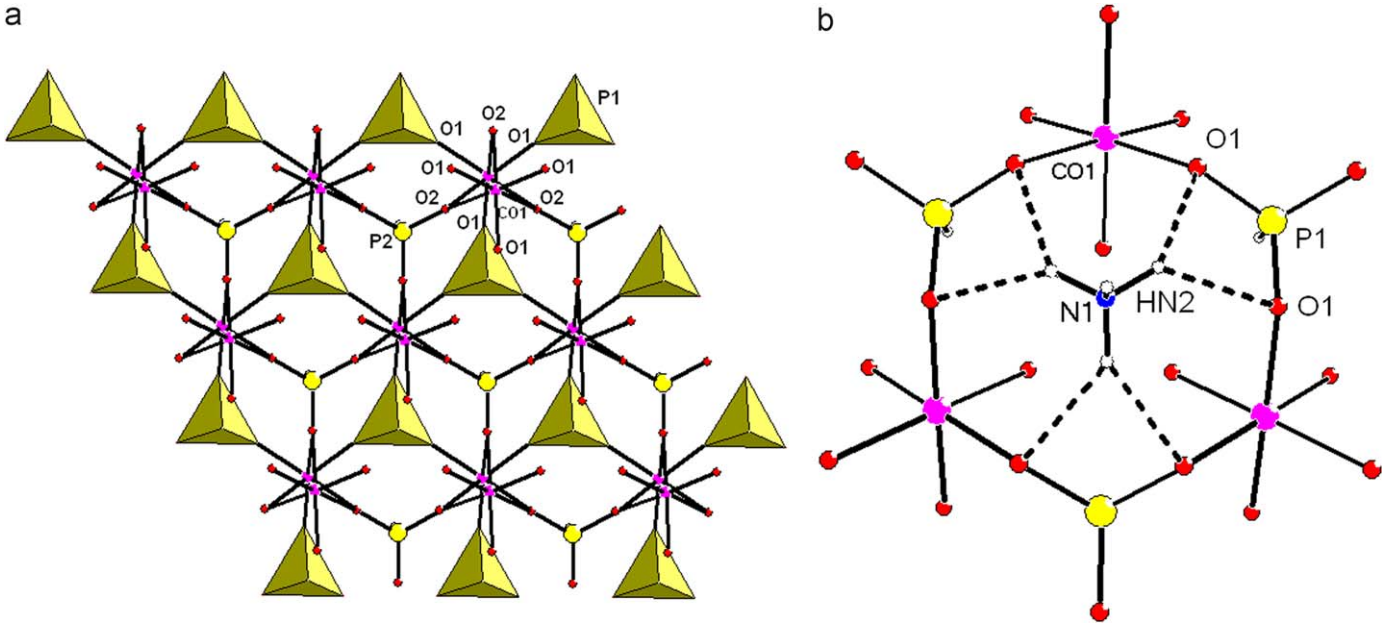

Fig. 4. The anionic complex sheet (a) and view of hydrogen bonds (b) in **2**. Color code: Co atoms, pink; P atoms, yellow; O atoms, red; N atoms, blue; the H atoms are open cycle. The dash lines represent hydrogen bonds. (For interpretation of the references to color in this figure legend, the reader is referred to the web version of this article.)

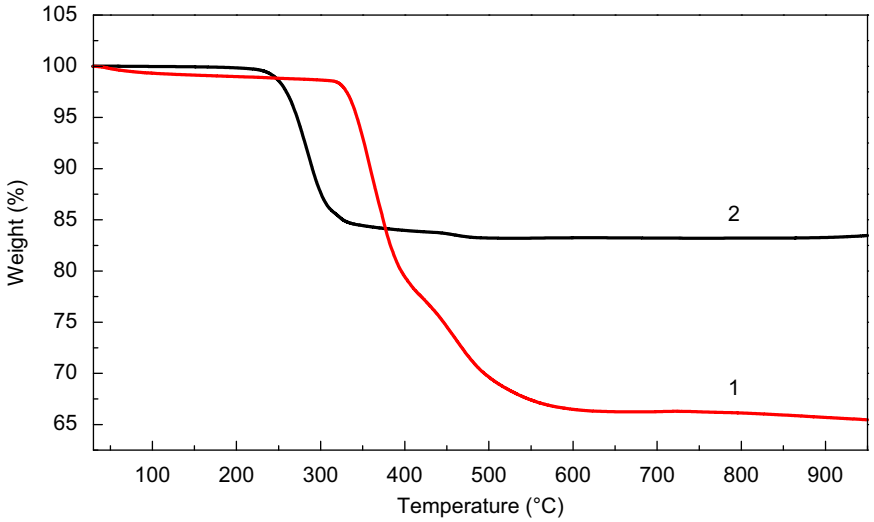

Fig. 5. Thermogravimetric analyses for **1** (red line) and **2** (black line). (For interpretation of the references to color in this figure legend, the reader is referred to the web version of this article.)

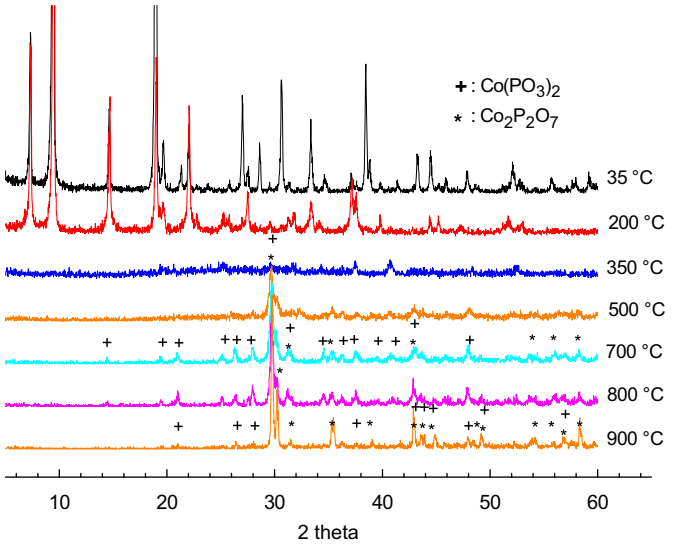

Fig. 6. Variable temperature powder X-ray diffraction for **2**. Mark code: +, those lines are present in the powder pattern of $Co(PO_3)_2$; *, those lines are present in the powder pattern of $Co_2P_2O_7$.

four-ring chains, have not been found in tetrahedron-based metal phosphites. When the MO_6 octahedra have been displayed in the structure to extend the inorganic framework, the presence of MO_6 unit will definitely facilitate the building of high dimensional framework. For example, compound **2** and some vanadium, [14] iron, [20] manganese, [30] or bimetal phosphates [12] are 2-D or 3-D structures that contain MO_6 octahedra.

A layered cobalt phosphate compound is strongly related to known 3-D trivalent metal phosphites $M_2(HPO_3)_3$ (M=Fe^{3+}, Ga^{3+}, Al^{3+}) [31,32] with building units that contain a dimmeric M_2O_9 unit. $M_2(HPO_3)_3$ (M=Fe^{3+}, Ga^{3+}, Al^{3+}) are composed of two face-shared MO_6 octahedra, which interlink nine phosphites tetrahedrally. However, the angle of the Co–O–Co (84.49°) in the Co_2O_9 of **2** is smaller than that in the corresponding $M_2(III)O_9$ (from 89.25° to 91.38°), because the repulsion between the divalent ions is small, while the angle of the O–Co–O (79.75°) in the Co_2O_9 of **2** is larger than that in the corresponding M_2(= 3 III)O_9 (from 74.45° to 76.10°).

Thermogravimetric analyses (*TGA*). A TGA experiment was performed in nitrogen stream at a heating rate of 10 °C/min using approximately 10 mg of samples **1** and **2**. One continuous weight loss step could be observed from 320 to 610 °C for **1**, as shown in Fig. 5. This weight loss is attributed to the sequential removal of organic amine (calc. 34.1%) and hydrogen gas (calc. 1.2%) by the dehydrogenation of phosphites. The total observed weight loss (34.5%) was consistent with the calculated value (35.3%) based on the above interpretation. After heating the sample **1** to 950 °C, powder X-ray diffraction was carried out to identify the solid residue $Co(PO_3)_2$ as the major phase, together with a small unidentified diffraction peak.

One continuous weight loss step could also be observed from 200 to 600 °C for **2**, as shown in Fig. 5. This weight loss is attributed to a complex chemical reaction. First, ammonia was removed from **2** by the decomposition of ammonium ion, and the proton from ammonium ion was donated to phosphites so that they converted into phosphorous acid. A self oxidation–reduction reaction of this phosphorous acid may have led to the formation of phosphine (PH_3) and phosphoric acid (H_3PO_4) above 200 °C [33]. The removal of ammonia (calc. 8.6%) and phosphine (calc. 8.6%) was consistent with the total observed weight loss (16.8%) after heating to 900 °C. The solid residue after heating was also identified as $Co(PO_3)_2$ and $Co_2P_2O_7$ by powder X-ray diffraction.

Temperature-dependent powder X-ray studies. To understand the structural information of **2** at various temperatures, temperature-dependent in situ XRD data were acquired from 30 to 900 °C, as shown in Fig. 6. The pattern at 30 °C was well consistent with the pattern simulated using the coordinates of the single-crystal study of **2**. At 200 °C, the pattern was similar to that at 30 °C. This indicates that the structure of **2** was thermally stable below 200 °C, since there was no weight loss from the TGA experiments. After the removal of ammonia and phosphine molecules, the crystal structure started to break down and became almost amorphous from 350 to 500 °C. From 700 to 900 °C, the XRD patterns showed the characteristic peaks of $Co(PO_3)_2$ (JCPDS 271120) and $Co_2P_2O_7$ (JCPDS 341378). At present, the phase exchange mechanism of **2** is unclear from 700 to 900 °C. We assume that the PO_3 group originates from phosphites in the compound, and the P_2O_7 group originates from a complex chemical reaction.

Magnetic properties. A Quantum Design SQUID magnetometer was used on powder samples to collect variable temperature magnetic susceptibility $\chi_M(T)$ data from 2 to 300 K in a magnetic

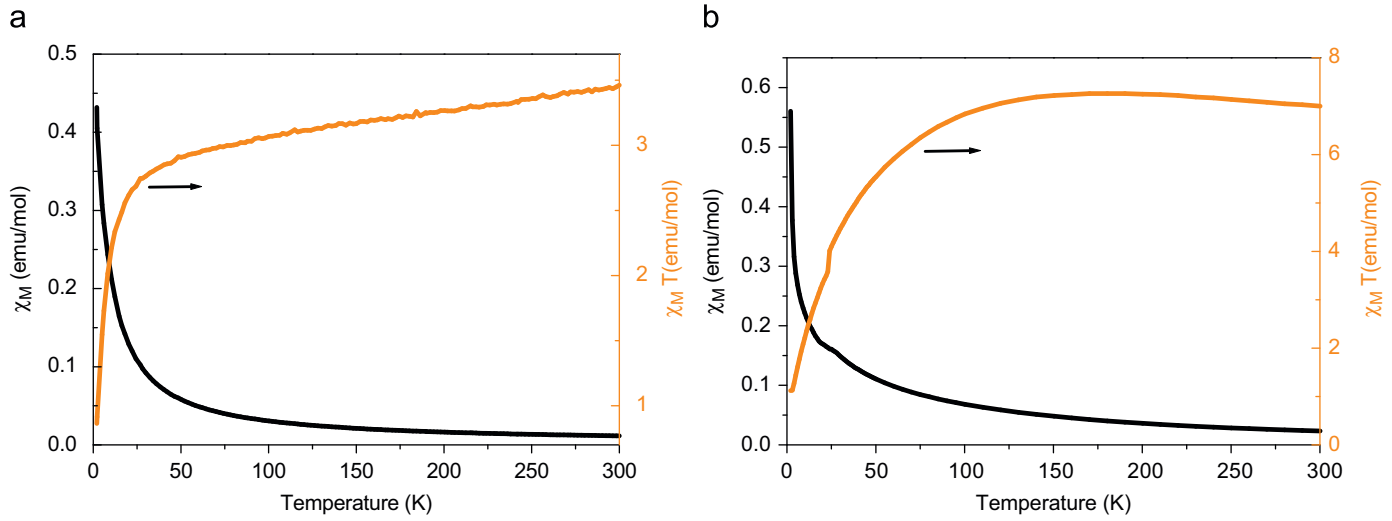

Fig. 7. Temperature dependence of χ_M and $\chi_M T$ values for **1**(a) and **2**(b).

field of 10 kOe, as shown in Fig. 7. The linear behavior of $1/\chi_M(T)$ above 50 K was in good agreement with the Curier–Weiss law, i.e., $1/\chi_M=(T-\theta)/C$(C=3.52 emu.K/mol and $\theta=-13.23$ K for **1** and C=7.05 emu.K/mol and $\theta=-9.85$ K for **2**). The negative value of the Weiss constant indicates antiferromagnetic near-neighbor superexchange between the Co ions. In **1**, magnetic coupling between cobalt ions occurs via phosphite superexchange pathways and is therefore expected to be weak. The magnetic property of **2** is apparently attributed to weak antiferromagnetic interactions between cobalt centers, as observed in the related octahedral Co(II) [24,34]. The obtained $\chi_M T$ products are indications that both compounds exhibit important orbit contributions at 300 K (5.16 μB for **1** and 5.31 μB for **2**). These behaviors correspond to the experimentally observed moments of high-spin Co(II) ions, with tetrahedral compound **1** exhibiting a smaller moment than octahedral compound **2**.

5. Conclusions

Secondary building units (SBUs) in the phosphites have been reported by Rojo's group. The structure of **1** comprises the most common 2T2t four-ring SBU and that of **2** comprises a rare 2O3t SBU. This result shows a large structural variety in cobalt phosphites. The magnetic properties of both these compounds are apparently attributed to weak antiferromagnetic interactions between cobalt ions.

Acknowledgments

This study was supported by the Far East University and National Science Council of the Republic of China (NSC 96-2113-M-269-001).

Appendix A. Supplementary material

Supplementary data associated with this article can be found in the online version at doi:10.1016/j.jssc.2009.10.029.

References

[1] [a] R.C. Haushalter, L.A. Mundi, Chem. Mater. 4 (1992) 31;
[b] M.I. Khan, L.M. Meyer, R.C. Hausshalter, A.L. Schweitzer, J. Zubieta, J.L. Dye, Chem. Mater. 8 (1) (1996) 43;
[c] K.-H. Lii, Y.-H. Huang, V. Zima, C.-Y. Huang, H.-M. Lin, Y.C. Jiang, F.-L. Liao, S.-L. Wang, Chem. Mater. 10 (1998) 2599;
[d] A. Choudhury, S. Natarajan, C.N.R. Rao, Chem. Commun. 1305 (1999);
[e] W.T.A. Harrison, L. Hannooman, J. Solid State Chem. 131 (1997) 363;
[f] S. Neeraj, S. Natarajan, C.N.R. Rao, Chem. Commun. 165 (1999);
[g] D. Chidambaram, S. Natarajan, Mater. Res. Bull. 33 (8) (1998) 1275;
[h] G.-Y. Yang, S.C. Sevov, J. Am. Chem. Soc. 121 (1999) 8389;
[i] J. Chen, R. Jones, S. Natarajan, M.B. Hursthouse, J.M. Thomas, Angew. Chem. Int. Ed. Engl. 33 (6) (1994) 639;
[j] S. Ekambaram, S.C. Sevov, Angew. Chem. Int. Ed. 38 (3) (1999) 372;
[k] M. Daniel, R.-M. Daniel, V. Jaume, Chem. Soc. Rev. 36 (2007) 770.
[2] [a] S. Oliver, A. Kuperman, G.A. Ozin, Angew. Chem., Angew. Chem. Int. Ed. Engl. 37 (1998) 46;
[b] C.N.R. Rao, S. Natarajan, S. Neeraj, J. Solid State Chem. 152 (2000) 302.
[3] S. Ekambaram, S.C. Sevov, J. Mater. Chem. 10 (2000) 2522.
[4] A. Choudhury, S. Natarajan, Solid State Sci. 2 (2000) 365.
[5] R.–K. Chiang, Inorg. Chem. 39 (2000) 4985.
[6] W.-K. Chang, C.-S. Wur, S.-L. Wang, R.-K. Chiang, Inorg. Chem. 45 (2006) 6622.
[7] W.-K. Chang, R.-K. Chiang, S.-L. Wang, J. Solid State Chem. 180 (2007) 1713.
[8] T. Rojo, J.L. Mesa, J. Lago, B. Bazan, J.L. Pizarro, M.I. Arriortua, J. Mater. Chem. 19 (2009) 1.
[9] F.-A. Sergio, J.L. Mesa, J.L. Pizarro, J.S. Garitaonandia, M.I. Arriortua, T. Rojo, Angew. Chem. Int. Ed. 43 (2004) 977.
[10] U.-C. Chung, J.L. Mesa, J.L. Pizarro, J.S. Marcos, J.S. Garitaonandia, M.I. Arriortua, T. Rojo, Inorg. Chem. 45 (2006) 8965.
[11] S. Mandal, M. Chandra, S. Natarajan, Inorg. Chem. 46 (2007) 7935.
[12] Y.-L. Lai, K.-H. Lii, S.-L. Wang, J. Am. Chem. Soc. 129 (2007) 5350.
[13] W. Fu, L. Wang, Z. Shi, G. Li, X. Chen, Z. Dai, L. Yang, S. Feng, Crys. Growth & Des. 4 (2004) 297.
[14] R.-K. Chiang, N.-T. Chuang, J. Solid State Chem. 178 (2005) 3040.
[15] L.E. Gordon, W.T.A. Harrison, Inorg. Chem. 43 (2004) 1808.
[16] J.A. Johnstone, W.T.A. Harrison, Inorg. Chem. 43 (2004) 4567.
[17] J. Fan, C. Slebodnick, D. Troya, R. Angel, B.E. Hanson, Inorg. Chem. 44 (2005) 2719.
[18] L. Chen, X. Bu, Inorg. Chem. 45 (2006) 4654.
[19] W.T.A. Harrison, R.M. Yeates, M.L.F. Phillips, T.M. Nenoff, Inorg. Chem. 42 (2003) 1493.
[20] W. Liu, H.-H. Chen, X.-X. Yang, J.-T. Zhao, Eur. J. Inorg. Chem. 946 (2005).
[21] S. Fernandez, J.L. Pizarro, J.L. Mesa, L. Lezama, M.I. Arriortua, T. Rojo, Int. J. Inorg. Mater. 3 (2001) 331.
[22] L. Zhao, J. Li, P. Chen, G. Li, J. Yu, R. Xu, Chem. Mater. 20 (2008) 17.
[23] J.-H. Liao, P.-L. Chen, C.-C. Hsu, J. Phys. Chem. Solids 62 (2001) 1629.
[24] J. Fan, G.T. Yee, G. Wang, B.E. Hanson, Inorg. Chem. 45 (2006) 599.
[25] Z.-E. Lin, W. Fan, F. Gao, N. Chino, T. Yokoi, T. Okubo, J. Solid State Chem. 179 (2006) 723.
[26] J. Liang, J. Li, J. Yu, Q. Pan, Q. Fang, R. Xu, J. Solid State Chem. 178 (2005) 2673.
[27] G.M. Sheldrick, SHELXTL Programs, Version 5.1; Brucker AXS, 1998.
[28] S. Oliver, A. Kuperman, A. Lough, G.A. Ozin, Chem. Mater. 8 (1996) 2391.
[29] R.-K. Chiang, J. Solid State Chem. 153 (2000) 180.
[30] S. Fernandez, J.L. Mesa, J.L. Pizarro, L. Lezama, M.I. Arriortua, R. Olazcuaga, T. Rojo, Chem. Mater. 12 (2000) 2092.
[31] R.E. Morris, M.P. Attfield, A.K. Cheetham, Acta Cryst. C 50 (1994) 473.
[32] P.M. Sghyar, J.D.L. Cot, M. Rafiq, Acta Cryst. C 47 (1991) 2515.
[33] A.G. Sharpe, Inorganic Chemistry, Longman Scientific & Technical, 1992, p. 356.
[34] V.B. Kusigerski, V.V. Spasojevic, N.D. Lazarov, D.S. Markovic, V.M. Matic, S.P. Sovilj, M. Guillot, Solid State Commun. 126 (2003) 319.